

This is a **peer-reviewed author manuscript version** of the article:

Bolognesi, S., Cecconet, D. & Callegari, A. Combined microalgal photobioreactor/microbial fuel cell system: Performance analysis under different process conditions. *Environmental Research*, vol. 192 (January 2021), art. 110263. DOI <https://doi.org/10.1016/j.envres.2020.110263>

The Published Journal Article is available at:

<https://doi.org/10.1016/j.envres.2020.110263>

© 2021. This manuscript version is made available under the CC-BY-NC-ND 4.0 license <https://creativecommons.org/licenses/by-nc-nd/4.0/>



1 **Combined microalgal photobioreactor/microbial fuel cell system: performance analysis under**
2 **different process conditions**

3

4 S. Bolognesi^{1,2,*}, D. Cecconet^{1,3}, A. Callegari¹ and A. G. Capodaglio¹

5 ¹ Department of Civil Engineering and Architecture, University of Pavia, Via Adolfo Ferrata 3,
6 27100 Pavia (Italy).

7 ² LEQUiA, Institute of the Environment, Universitat de Girona, 69, M^a Aurèlia Capmany, Girona
8 17003, Spain

9 ³ Department of Chemistry, University of Pavia, Viale Taramelli 12, 27100 Pavia (Italy)

10

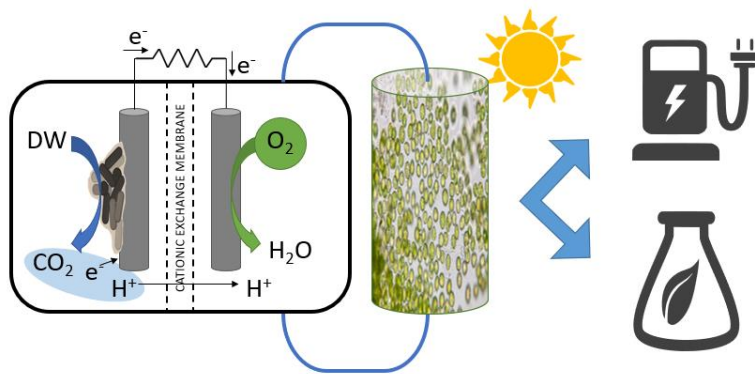
11 *corresponding author; Email: silvia.bolognesi@unipv.it Address: Department of Civil Engineering
12 and Architecture, University of Pavia, Via Adolfo Ferrata 3, 27100 Pavia (Italy). Phone: +39 0382
13 985762

14

15

16 **Abstract**

17 Increasing energy demands and greenhouse gases emission from wastewater treatment processes
18 prompted the investigation of alternatives capable to achieve effective treatment, energy and materials
19 recovery, and reduce environmental footprint. Combination of microbial fuel cell (MFC) technology
20 with microalgal-based process in MFC-PBR (photobioreactor) systems could reduce GHG emissions
21 from wastewater treatment facilities, capturing CO₂ emitted from industrial facilities or directly from
22 the atmosphere. Microalgae production could enhance recovery of wastewater-embedded resources.
23 Two system MFC-PBR configurations were tested and compared with a control MFC, under different
24 operating conditions, using both synthetic and agro-industrial wastewater as anolytes. COD removal
25 efficiency (η COD) and energy production were monitored during every condition tested, reaching
26 η COD values up to 99%. Energy recovery efficiency and energy losses were also evaluated. The
27 system equipped with microalgal biocathode proved to be capable to efficiently treat real wastewater,
28 surpassing the effectiveness of the control unit under specific conditions. Oxygen provided by the
29 algae improves the overall energy balance of this system, which could be further enhanced by many
30 possible resources recovery opportunities presented by post-processing of the cathodic effluent.



31

32

33 **Keywords**

34 *Chlorella*; Bioelectrochemical Systems; CO₂ recovery; Renewable energy; Wastewater treatment;
35 Biorefinery

36 This research did not receive any specific grant from funding agencies in the public, commercial, or
37 not-for-profit sectors.

38

39

40

41

42 **1. Introduction**

43 Fossil fuels combustion and CO₂ emissions from anthropic activities contribute to ongoing climate
44 change effects, with the first decade of the new millennium registered as the warmest ever (Arndt et
45 al., 2010). At the same time, water systems, including wastewater treatment facilities, have been
46 indicated among major energy consumers at municipal level worldwide (Rosso and Stenstrom, 2008).
47 It was estimated that they alone may require 1-3% of the total electrical energy output of a country
48 (US DOE, 2014). Current wastewater treatment state-of-the-art technology requires energy
49 consumption between 20 and 45 kWh/PE-year (population equivalent), consequently, it is not only
50 highly energy intensive, but also a significant sources of greenhouse gas (GHG) emissions (Sabba et
51 al. 2018), whose reduction has been recently mandated by European Union and other countries'
52 policies. Energy savings and wastewater valorization by exploitation of its residual resources content,
53 may provide significant contribution to Circular Economy and GHGs reduction (Capodaglio and
54 Olsson, 2020). Based on current knowledge, novel concepts of biorefinery could be developed to
55 satisfy the need of more sustainable environmental protection technology and, at the same time,
56 recover necessary energy and resources (Cherubini, 2010).

57 Microbial fuel cells (MFCs) are a promising technology for wastewater treatment, characterized by
58 electrical energy recovery coupled with low greenhouse gases (GHG) emissions and reduced sludge
59 production (Capodaglio et al., 2013). MFCs convert the chemical energy of organic pollutants
60 (substrate) directly into electrical energy, catalytic activity of electrochemically active bacteria (EAB)
61 (Logan et al., 2006; Molognoni et al., 2018), potentially achieving higher conversion efficiency (44%)
62 than a conventional anaerobic treatment (28%) (Luo et al., 2017; McCarty et al., 2011).

63 In MFCs, bacteria at the anode oxidize organic substrates producing CO₂, protons and electrons;
64 electrons flow through an external circuit to the cathode, producing electrical energy and closing the
65 redox reaction (Capodaglio et al. 2015). Energy production is limited, among many factors, by the
66 availability of a terminal electron acceptor (TEA) at the cathode, most commonly, oxygen (Bolognesi
67 et al., 2020). CO₂ is released by oxidative treatment of organic matter and is also

68 contained in MFC anodic effluents; its sequestration could be helpful to decrease global CO₂
69 emissions, even at low emission rates, whenever feasible. Recently, the use of microalgae for co-
70 treatment of wastewater was proposed, being an effective process for both resources recovery and
71 CO₂ sequestration (Gabriel et al., 2018; Wang et al., 2010).

72 Microalgae, on the other hand, are well known as potential candidates as feedstock in biorefineries
73 (third generation feedstocks) for biofuels and biomaterial production. They can in fact generate
74 recovered raw materials more sustainably than first and second generation feedstocks, with lower
75 land footprint and no food crops competition issues (Callegari et al., 2020; Chew et al., 2017). They
76 contain lipids, minerals, carbohydrates and proteins that could be elaborated into valuable products,
77 such as biofuels, primary chemicals, food, livestock and aquaculture feed and other value-added
78 products (Kothari et al., 2017). Microalgae also contribute to CO₂ emissions reduction, due to their
79 photosynthetic nature. Microalgae can be grown under different conditions: open ponds, closed
80 reactors (such as photobioreactors, PBR) and in different types of water, including nutrient-rich
81 wastewater (Richmond, 2004).

82 Combining MFC technology with algal metabolism, e.g. by coupling a PBR to a MFC cathode, could
83 be an advantageous process improvement: (i) achieve sustainable wastewater treatment (carbon and
84 nutrients removal) by an emerging green technology, MFCs, with low gaseous emission and low
85 solids production, and consequently reduced sludge production (Logan and Rabaey, 2013); (ii) energy
86 recovery by direct conversion of chemical energy in electrical energy (Capodaglio et al., 2016); (iii)
87 CO₂ capture by microalgae with conversion into process-required TEAs and oxygen (Jiang et al.,
88 2013); (iv) production of biofuels or valuable recovered materials from algal process residuals
89 (Brennan and Owende, 2010; Goglio et al., 2019). It is important to point out that in such scheme,
90 microalgae could equally capture anode-produced CO₂, or alternatively utilize gaseous effluents
91 originated from an industrial facility, or atmospheric CO₂, converting it into oxygen (Wang et al.,
92 2019). Some authors explored the possibility of enhancing nutrients removal by using algal
93 biocathodes (Nguyen and Min, 2020). Based on these premises, interest on MFC-PBR systems has

94 increased in the latter years amongst the research and professional communities (Cui et al., 2014; Do
95 et al., 2018; Gouveia et al., 2014; Khazraee Zamanpour et al., 2017).
96 Light/dark cycles influence O₂ production, growth rate and algal stress of these processes, and
97 consequently may affect both bioelectricity production and possible recovery products from the
98 effluent, affecting the global energy and economic balance of the system (León-Vaz et al., 2019).
99 This study evaluates the influence of lighting conditions and electron acceptor supply in an MFC-
100 PBR unit operated both on synthetic substrate (acetate) and real agro-industrial wastewater as anodic
101 feed, in long-term operation (4 months). Energy losses were evaluated under two different aeration
102 conditions in the second part of the study, to highlight how TEA availability affects system
103 performance.

104

105 **2. Materials and methods**

106 *2.1 Experimental setup and operation*

107 Two identical double-chamber MFCs (MFC1 and MFC2, respectively) were built and operated as
108 described by Cecconet et al. (2018). Each MFC consisted of an anodic and a cathodic chamber, both
109 filled with 800 g of granular graphite (diameter 1.5-5 mm, model 00514, EnViroCell, Germany),
110 decreasing the free volume to 430 mL net anodic (NAC) and cathodic (NCC) compartment. The two
111 chambers are separated by a cationic exchange membrane (CEM, CMI-7000, Membranes
112 International Inc., USA). A graphite rod (250 x 4 mm, Sofacel, Spain) was used as electron collector.
113 The external electrical circuit was closed by using a 33 Ω resistance as a load. This value was assumed
114 to be as close as possible to the static internal resistance of the system, as confirmed by polarization
115 curves operated on the system and reported in previous works (Molognoni et al., 2018, 2014).
116 The study herein reported was divided into two phases, according to variations of system
117 configuration. In the first phase, two different anolytes were tested: acetate solution (1 g L⁻¹) during
118 period I, then dairy wastewater (DW, collected periodically from a nearby cheese factory) in period
119 II. These were fed continuously, at flow rate of 1 L d⁻¹. In the second phase, only DW was fed to the

120 units. Characteristics of DW varied throughout the study following the production schedule at the
 121 factory. DW was stored at 4°C until use to limit bacteria activity, and then fed to the system using
 122 collapsible 10 L jerry cans to limit contact with the atmosphere. Table 1 summarizes anolyte
 123 characteristics during the study.

124

125 **Table 1** – Summary of the characteristics of the influents used throughout the study.

| Substrate | Test | Anodic influent | | | Cathodic influent | | |
|--------------|---------|-----------------|-------------------------------------|--|-------------------|-------------------------------------|------|
| | | pH | Conductivity [mS cm ⁻¹] | COD _{IN} [mgCOD L ⁻¹] | pH | Conductivity [mS cm ⁻¹] | |
| First phase | Acetate | 1 | 7.80 | 1.02 | 553 | 7.99 | 3.07 |
| | | 2 | 7.47 | 0.99 | 529 | 7.67 | 3.01 |
| | | 3 | 7.54 | 1.16 | 544 | 7.76 | 2.96 |
| | | 4 | 8.10 | 1.03 | 528 | 8.05 | 2.70 |
| | | 5 | 7.78 | 1.18 | 568 | 8.19 | 3.25 |
| | | 6 | 7.71 | 1.01 | 527 | 8.02 | 3.09 |
| | DW | 7 | 7.90 | 0.86 | 426 | 7.97 | 4.65 |
| | | 8 | 8.07 | 1.12 | 946 | 7.97 | 3.47 |
| | | 9 | 7.34 | 0.78 | 707 | 7.83 | 3.56 |
| | | 10 | 7.62 | 1.07 | 1032 | 7.82 | 2.08 |
| | | 11 | 8.03 | 3.34 | 918 | 7.81 | 3.38 |
| | | 12 | 9.25 | 3.15 | 1174 | 8.14 | 2.84 |
| Second phase | DW | 1 | 7.10 | 0.66 | 1241 | 7.97 | 3.02 |
| | | 2 | 7.25 | 0.86 | 1195 | 8.12 | 2.95 |
| | | 3 | 7.12 | 0.78 | 1142 | 7.85 | 2.88 |
| | | 4 | 7.85 | 0.76 | 742 | 8.13 | 2.79 |
| | | 5 | 8.76 | 0.92 | 652 | 8.17 | 3.03 |
| | | 6 | 9.39 | 0.77 | 374 | 7.99 | 3.15 |
| | | 7 | 8.45 | 1.44 | 952 | 7.84 | 2.18 |
| | | 8 | 7.48 | 2.05 | 1261 | 7.94 | 2.25 |
| | | 9 | 7.73 | 1.53 | 390 | 7.90 | 1.63 |
| | | 10 | 7.83 | 2.64 | 1163 | 8.02 | 3.10 |
| | | 11 | 7.66 | 1.67 | 606 | 8.24 | 2.65 |
| | | 12 | 6.31 | 1.57 | 1195 | 7.54 | 1.58 |

126

127 A similar feeding mode was adopted for the cathodic chambers, fed with a phosphate buffer solution
 128 (PBS, 10 mM, pH 7) containing macroelements and an inorganic source of carbon (507 mg L⁻¹
 129 NaH₂PO₄, 819 mg L⁻¹ Na₂HPO₄, 1000 mg L⁻¹ NaHCO₃, 130 mg L⁻¹ KCl, 310 mg L⁻¹ NH₄Cl, modified

130 from Xia et al., (2013)). In MFC2 recirculation of the effluent from the PBR was also returned to the
131 cathode, as explained in Section 2.2. An internal recirculation loop was activated in each chamber to
132 achieve well mixed conditions within.

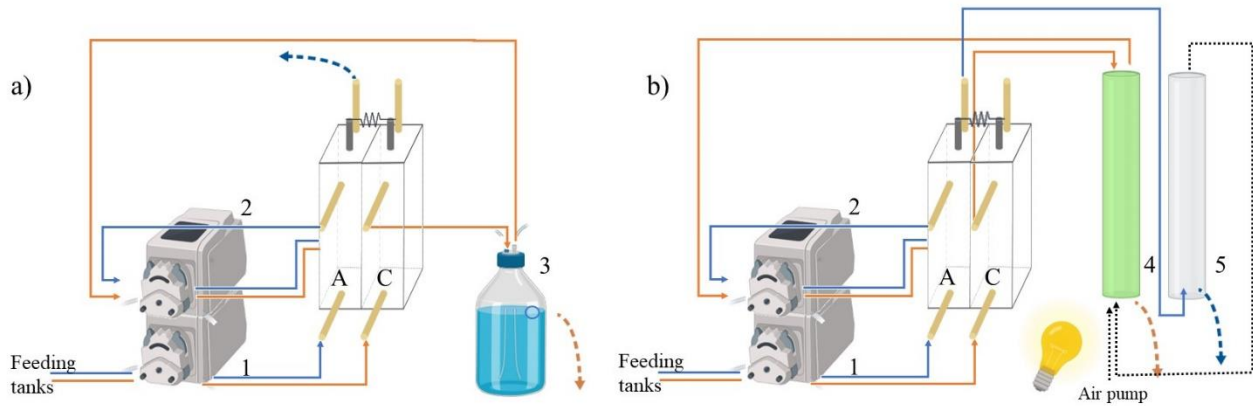
133

134

135 *2.2 First phase*

136 During the first phase of the study, both MFCs were operated for 60 days, 32 using acetate as
137 substrate, 28 using undiluted raw DW; MFC2 was coupled with the PBR, while MFC1 was
138 individually operated as control. This phase was sub-divided in two separate periods, each
139 corresponding to a different substrate used as anolyte for the MFCs: synthetic wastewater (acetate)
140 in period I, DW in period II. Oxygen (from air) was selected as electron acceptor, introduced
141 according to two different methods in the two MFCs. In the MFC2 setup, a PBR unit consisting of
142 two methacrylate tubular reactors ($d=0.03$ m, $h=0.3$ m) and containing a mixed culture of microalgae
143 (*Chlorella*) was operated in the cathode recirculation line. Microalgae *Chlorella* converted CO_2
144 (captured from the atmosphere or from the gaseous effluent produced by the anode) into oxygen
145 during daytime. Two different configurations for MFC2's TEA supply were tested during the study:
146 PBR-aerated (PBR-air) configuration, with a fish tank air pump connected to the PBR via an aeration
147 buffer unit to introduce ambient air (CO_2 for conversion, and O_2); and CO_2 -capture configuration, in
148 which the PBR was attached to a gas phase separator receiving both liquid and gaseous effluent from
149 the anodic chamber, exploiting the anodic bacterial produced biogas containing CO_2 . Gas phase was
150 pushed to the cathodic chamber by the increasing volume of liquid effluent in the methacrylate tube.
151 PBR light source consisted of a conventional led bulb (40 W). Cathode effluent was collected from
152 an overflow device in the topmost section of the PBR. MFC1, acting as experimental control, was
153 equipped with an aeration buffer in in the cathodic recirculation loop, to obtain an oxygen-saturated
154 catholyte. The exhausted catholyte was expelled from the system via an overflow in the same buffer.
155 In either case, the ensemble of cathode plus aeration buffer/PBR will be referred to, from now on, as

156 “cathode system”. *Chlorella* was cultivated into an external reactor, and changed in the PBR every
 157 9-10 days (two feeding cycles). The complete experimental setup is illustrated in Figure 1.



158
 159 **Figure 1** – Experimental setup configuration in the first phase. (a) MFC1 with aeration buffer. (b):
 160 MFC2 setup with PBR. A: Anode. C: Cathode. R_{ext} : External resistor. (1) Feeding pump; (2)
 161 recirculation pumps; (3) aeration buffer; (4) photobioreactor (PBR); (5) CO₂ separator. Orange lines:
 162 anodic chamber feeding and recirculation line. Blue lines: cathodic chamber feeding and recirculation
 163 line. Black dotted lines: air supply. Dashed lines: effluent discharge.

164
 165 PBR performance in MFC2 was evaluated under six different conditions for each period, by varying
 166 lighting conditions (light/dark ratio 16/8, 12/12, 24/0) and CO₂ supply conditions (PBR-air and CO₂-
 167 capture), while MFC1 was operated as a control throughout the experiment with the same substrate.
 168 Each test lasted 4-5 days, and all tests were executed in succession. A summary of the operational
 169 conditions operated during the first phase is reported in Table 2.

170
 171 **Table 2** - Operational conditions throughout the first phase of the experimentation for MFC2. DW:
 172 dairy wastewater

| Test | Substrate | CO ₂ source | Light/dark ratio |
|------|-----------|------------------------|------------------|
| 1 | Acetate | PBR-Air | 16/8 |

| | | | |
|----|----|--------------------------|-------|
| 2 | | CO ₂ -Capture | 16/8 |
| 3 | | PBR-Air | 12/12 |
| 4 | | CO ₂ -Capture | 12/12 |
| 5 | | PBR-Air | 24/0 |
| 6 | | CO ₂ -Capture | 24/0 |
| 7 | DW | PBR-Air | 16/8 |
| 8 | | CO ₂ -Capture | 16/8 |
| 9 | | PBR-Air | 12/12 |
| 10 | | CO ₂ -Capture | 12/12 |
| 11 | | PBR-Air | 24/0 |
| 12 | | CO ₂ -Capture | 24/0 |

173

174

175

2.3 Second phase

176

During the second phase of the study the two systems were configured as shown in Figure 2: raw DW

177

was fed as anolyte, as in the first phase of the study; both systems cathodes were coupled to a PBR,

178

containing microalgae, applying the best dark/light condition (16/8) determined in the first phase, but

179

with different TEA supply conditions. MFC1 was operated under PBR-air mode, while MFC2 was

180

equipped with the CO₂-capture system. Each test cycle lasted 5 days (except for two cycles lasting

181

only 4 days), for a total duration of 58 days (12 cycles). The aim of the second phase was to highlight

182

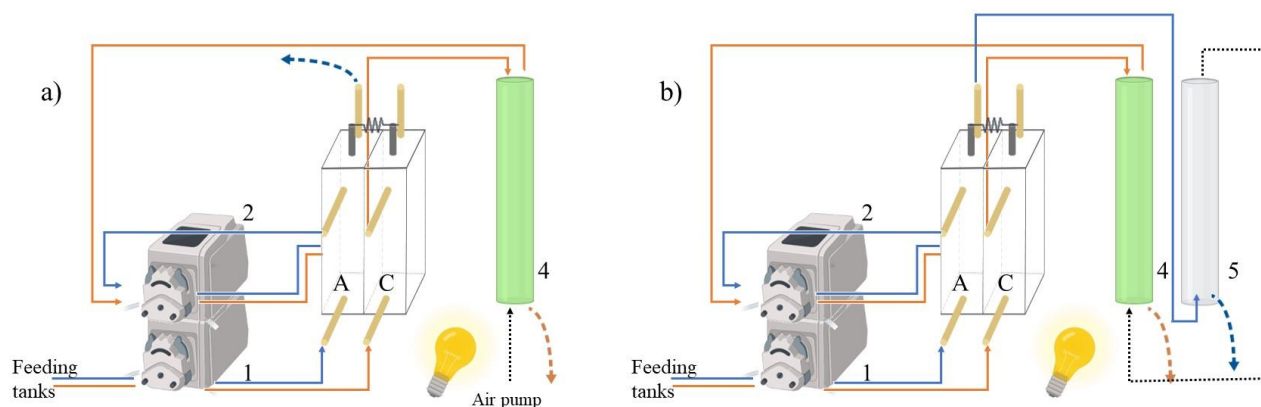
the different performance of the two systems under the same conditions and characteristics, except

183

for the TEA-supply method. During this phase, energy losses of the two MFC-PBR systems were

184

evaluated to determine advantages and drawbacks of each configuration.



185

186 **Figure 2** – Experimental setup configuration in the second phase. (a) MFC1 under PBR-air
 187 configuration. (b): MFC2 under CO₂-capture configuration. A: Anode. C: Cathode. R_{ext}: External
 188 resistor. (1) Feeding pump; (2) recirculation pumps; (3) aeration buffer; (4) photobioreactor (PBR);
 189 (5) CO₂ separator. Orange lines: anodic chamber feeding and recirculation line. Blue lines: cathodic
 190 chamber feeding and recirculation line. Black dotted lines: air supply. Dashed lines: effluent
 191 discharge.

192

193

2.4 Data analysis and evaluation

194 Anodic potentials were monitored with an Ag/AgCl reference electrode (+197 mV vs Standard
 195 Hydrogen Electrode, Xi'an Yima Opto-electrical Technology Co., China) and recorded at 1-min
 196 intervals by an automatic data acquisition system (NI USB-6008, National Instruments Italy, Milan)
 197 connected to a PC. Overall MFC potentials were recorded with the same time interval, power (P) was
 198 determined from continuous current (I) and voltage measurement (V). Current (dI) and power (dP)
 199 densities were then calculated dividing the respective value of I and P by the NAC volume of each
 200 compartment. Anodic coulombic efficiency (CE) was computed as described in Ceconet et al.
 201 (2018). Determination of effluent COD (one sample per MFC per test) and acetate/wastewater
 202 influent COD (one common sample for every feed bag refill) was performed using a
 203 spectrophotometer (HI83224 Wastewater Treatment Photometer, Hanna Instruments, Italy). Organic

204 matter removal efficiency (η_{COD} - %) was determined as described in Molognoni et al. (2014).
205 Conductivity and pH were measured at least once during every test for both anode and cathode
206 influents and effluents (IntelliCALTM probes + HQdTM Digital Meter, Hach Lange, Italy).
207 The normalized energy recovery (NER) of the MFCs, a parameter that expresses the amount of energy
208 recovered per removed mass of COD (NER_S , kWh kg_{CODrem.}⁻¹) and per volume of treated wastewater
209 (NER_V , kWh m⁻³_{treated}) was calculated for each period and for the total experiment with the following
210 equations, as proposed in Ge et al. (2014):

$$211 \quad \text{NER}_V = \frac{P \cdot t}{V_{\text{treated}}} \quad (1)$$

$$212 \quad \text{NER}_S = \frac{P \cdot t}{\text{kg}_{\text{CODremoved}}} \quad (2)$$

213

214 Energy loss factors were calculated, corresponding to each available polarization curve, using the
215 energy balance equation with the methodology reported by Molognoni et al. (2014). In particular,
216 anode and cathode overpotentials (η_{An} and η_{Cat}), ionic (E_{ionic}), pH gradient ($E_{\Delta\text{pH}}$) and membrane
217 transport losses (E_t) were evaluated. Ohmic losses other than ionic were not directly measured, but
218 included in the terms η_{An} and η_{Cat} (Sleutels and Hamelers, 2009).

219

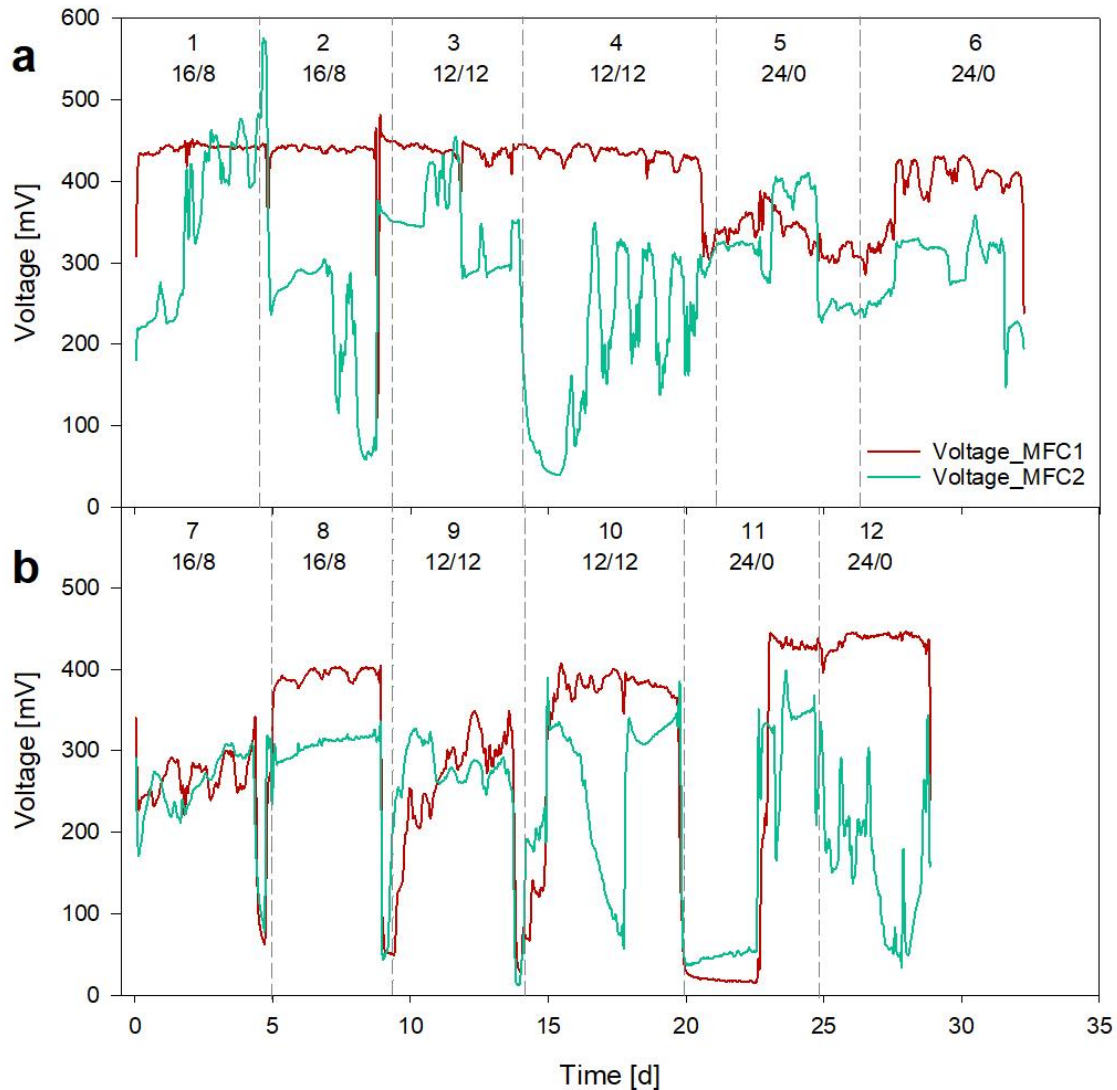
220 **3. Results and discussion**

221 Results for the first and second phases are presented separately, since each one focused on a different
222 specific aspect. The aim of the first phase was to evaluate the system's energy recovery performance
223 and substrate conversion efficiency, by using both synthetic and real wastewater, under different
224 conditions. During the second phase, where MFCs were fed only with DW, evaluation of PBR CO₂
225 conversion efficiency was the main focus.

226

227 *3.1 Electrical production*

228 The first operational period was characterized by the use of a synthetic substrate as anodic feed.
229 Organic loading rate (OLR) was nearly constant during this phase ($1.25 \pm 0.06 \text{ kgCOD m}^{-3} \text{ d}^{-1}$),
230 lasting 32 days. Figure 3a shows voltage generated by the two MFCs during tests I-VI.
231 MFC1 showed constant electricity production throughout this phase, due to the simple characteristics
232 of the treated substrate, achieving an average voltage of $409.71 \pm 46.10 \text{ mV}$ (corresponding to a
233 current density of $28.28 \pm 2.57 \text{ A m}^{-3}$). MFC2 performance overall was less stable, and more
234 susceptible to variability in different feeding periods due to changes of cathodic conditions. It can be
235 noted that alternation of light and darkness influenced electric production, due to varying availability
236 of oxygen as cathodic TEA. Generally, direct atmospheric O_2 supply led to better performances (as
237 shown in tests 1, 3, 5) than supply of captured anode-produced CO_2 and subsequent conversion into
238 O_2 by algae: in the former case, difference between day/night conditions were detectable, but not
239 inducing large variations in electricity production, with electrical performance presenting an overall
240 increasing trend. During test I and V, electricity production of MFC2 overtook MFC1, achieving the
241 highest voltage of the whole experimentation (573.92 mV). Test under CO_2 -capture conditions (2, 4,
242 6) instead, were more likely influenced by the activity of algae at the biocathode, and presented high
243 voltage drops during night-time, and an overall lower energy production. Light/dark alternation
244 periods seems to influence both availability of TEA and algal stress, resulting in optimal oxygen
245 production with the 16/8 sequence in the atmospheric-aerated test. As for the CO_2 -capture
246 configuration, the best electric production was achieved with the 24/0 sequence, although increased
247 algal stress by constant lighting caused a big voltage drop in day 31. Stress conditions for algae entail
248 metabolic changes, affecting metabolic rates. In this case, stress limited photosynthetic activity
249 efficiency in the long run.
250
251



252

253 **Figure 3** - Voltage from MFC1 and MFC2 in the first phase of the experimentation a) with acetate
 254 feed; b) with dairy wastewater. Light/dark ratios for MFC2 are reported in the graph. Odd numbers:
 255 PBR-air configuration; even numbers: CO₂-capture configuration.

256

257 As for period II, during which the MFCs were fed with DW, results are more difficult to interpret,
 258 due to the variability of the influent itself, and hydrodynamic issues related to the nature of DW,
 259 frequently causing obstructions in the feeding line, which required extra maintenance (Ceconet et
 260 al., 2018). Figure 3b shows the voltage profile observed in period II. Although the absolute value of
 261 current produced was lower, the voltage gap observed between MFC2 and control MFC1 decreased;
 262 in tests 7, 9 and 11 (PBR-air configuration) the two profiles are very close. In CO₂-capture

263 configuration tests (8, 10, 12) the gap is still high, especially in test 12, with algal stress causing
264 voltage drop earlier than in the corresponding test with acetate. Comparing average voltage measured
265 during periods I and II in the two MFCs, a voltage drop due to the change from synthetic to real
266 wastewater in the control experiment is obvious: MFC1 accounted for 387.60 ± 85.65 mV in period
267 I, against 290.24 ± 130.46 mV, when using DW as anolyte, with difference of about 100 mV. A
268 different behavior is observed for MFC2, with average voltage of 286.77 ± 102.53 measured in period
269 I, and of 236.77 ± 97.53 mV in period II. Comparing performance in terms of generated voltage for
270 the two systems in each period, it is evident that MFC1 energy production in period I was significantly
271 higher, while the difference with DW as anolyte between the two systems is not that relevant. When
272 using an easily biodegradable substrate, such as acetate, electron transfer efficiency is limited by
273 cathode TEA availability only. This is obviously lower in MFC2 since it depends on light availability,
274 and algae respiration during night-time. It is encouraging, however, the gap reduction when using
275 real wastewater as substrate: substrate complexity in fact slows down the anodic reactions, limiting
276 the amount of electrons released by substrate degradation, and consequently reducing the limiting
277 influence of microalgal metabolism on cathodic activity.

278 In the second phase, microalgae were applied at both cathode systems, under a 16/8 light/dark
279 sequence and DW feed. Under PBR-air configuration, the performance of MFC1 showed higher
280 variability in generated voltage and, overall, lower current productions were observed in both MFCs.
281 Average MFC1 voltage throughout the whole phase was 299.34 ± 133.91 mV (corresponding to an
282 average current density of 20.61 ± 9.27 A m⁻³). The difference with MFC2 (in CO₂-capture
283 configuration) was lower, because the main factor that affected electricity production was the nature
284 of the substrate. MFC2 achieved an average voltage of 231.42 ± 98.70 mV, corresponding to a current
285 density of 15.91 ± 6.83 A m⁻³. Voltage monitored in this phase of the Study is reported in Figure S1
286 (supplementary information).

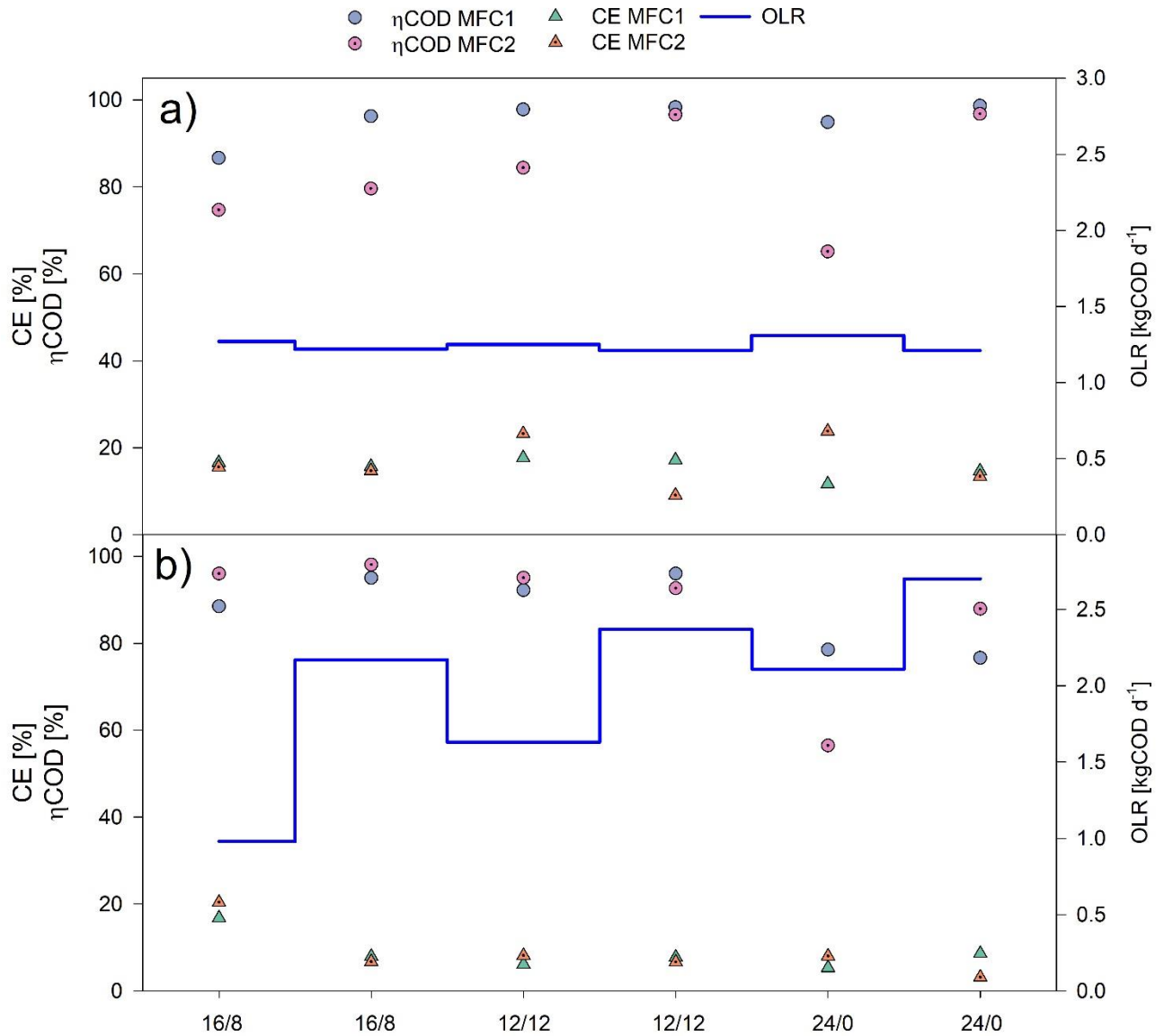
287

288

3.1 Organic matter removal efficiency and energy efficiency

289

290 Organic matter removal (η COD) was evaluated throughout the study. MFC1 and MFC2 showed
291 similar behavior in terms of organic matter removal efficiency, with slightly better performance by
292 MFC1, achieving COD removal of $91 \pm 8\%$ against $85 \pm 14\%$ of MFC2 (Figure 4). With acetate as
293 influent, COD removal efficiency of MFC1 overcame the one obtained by MFC2 (Table 3), while
294 the opposite happened with DW as a feed, where MFC2 achieved the best results, except for test 11,
295 in which the lowest organic matter removal efficiency (56 %) was observed. CE varied throughout
296 the study, depending on the influent feed, and on the TEA supply method, with slightly better results
297 for MFC2. CE of both systems was higher when using acetate as a substrate rather than in the case of
298 DW anolyte: its highest values (17.2–17.7% for MFC1, 23.2–23.8% for MFC2) were obtained with
299 this substrate. The best results in MFC2 operation were achieved in tests under PBR-air mode, due to
300 greater TEA availability at the cathode (Test III and V). The same trend was seen also in test with
301 DW as influent, where PBR-aeration tests overcame CO₂-capture tests in terms of CE values. In PBR-
302 air configuration MFC2's CE was even higher than MFC1's. The lowest CEs (5.3% for MFC1 in
303 Test 11, 3.2% for MFC2 in Test 12) were observed with DW as feed, for both MFCs. For MFC2, this
304 value confirmed the low efficiency of continue lighting. While OLR in acetate-feed tests was
305 constant, in DW tests OLR variability was dependent on variable substrate characteristics. Tests under
306 DW feed were generally characterized by higher OLR (average: 2.09 kgCOD d⁻¹); observed results
307 confirmed reports from previous studies: in presence of high OLR, MFCs tend to develop
308 methanogenic biomass, competitive to EABs, which leads to higher COD removal efficiency, while
309 decreasing MFC's electric efficiency (Molognoni et al., 2016). Results concerning the second phase
310 have been reported extensively in SI, figure S3. Methanogens also consume organic substrate,
311 increasing the overall COD removal of the system. The present study achieved comparable results in
312 terms of CE and better results in terms of η COD (up to 10% more) than previous experiences of the
313 group on similar substrate, operating in the same configuration as MFC1 in the first phase, meaning
314 that the addition of microalgae improved systems' efficiency (Ceconet et al., 2018).



315

316 **Figure 4** – OLR, COD removal and CE for MFC1 and MFC2 throughout the first phase of the
 317 study: a) acetate; b) DW. MFC acted as a control with no microalgae in the system.

318

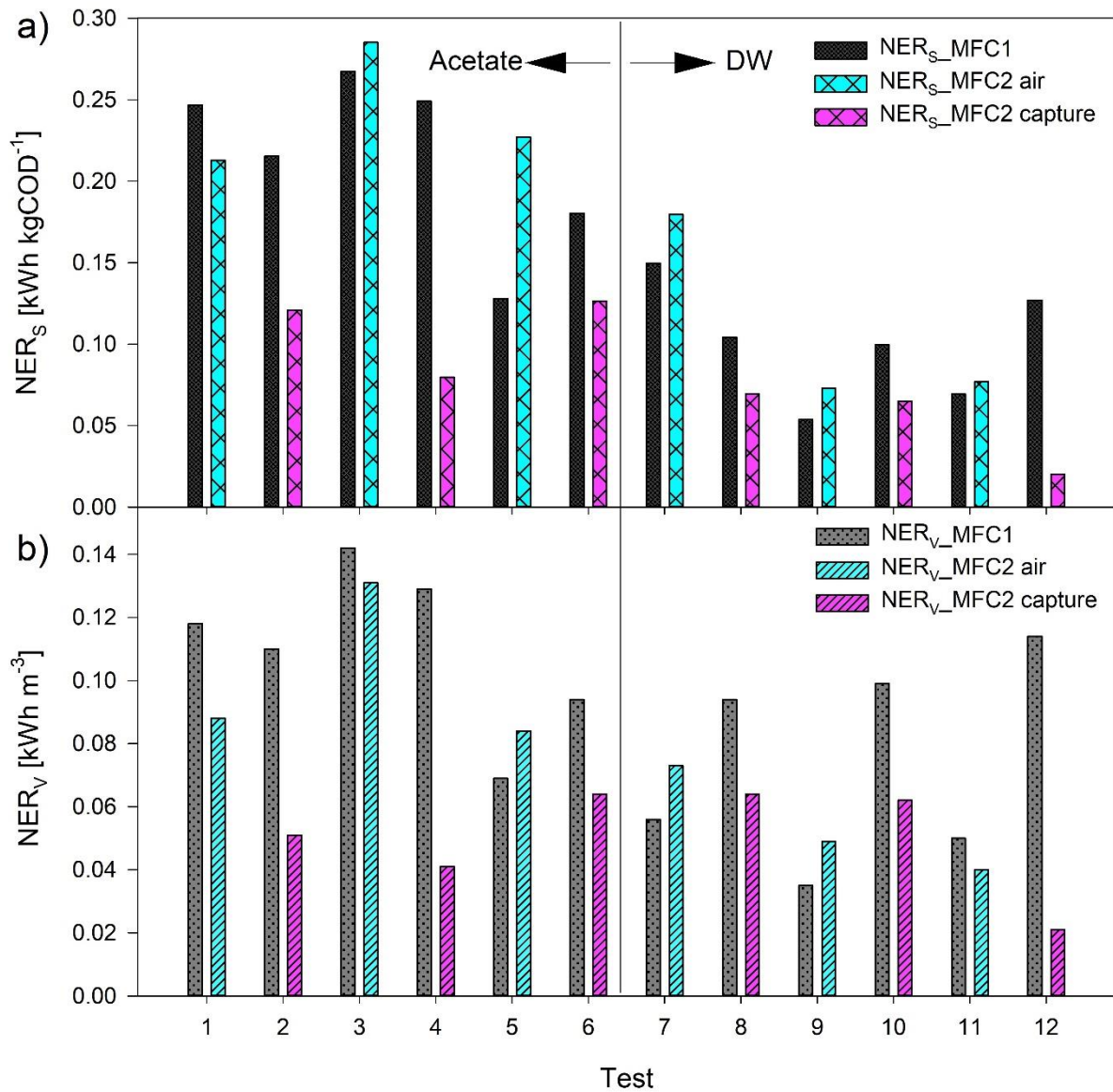
319 **Table 3** - Values of η_{COD} , CE, NER_v and NER_s under different substrate and TEA supply
 320 conditions in period I.
 321

| Substrate | Mode | MFC1 | | | | MFC2 | | | |
|-----------|---------|-------------------------|------------------|--|---|-------------------------|------------------|--|---|
| | | η_{COD} (%) | CE (%) | NER_v (kWh m^{-3}) | NER_s ($\text{kWh kgCOD}_{\text{rem}}^{-1}$) | η_{COD} (%) | CE (%) | NER_v (kWh m^{-3}) | NER_s ($\text{kWh kgCOD}_{\text{rem}}^{-1}$) |
| Acetate | Air | 93.10 ± 5.79 | 15.32 ± 3.21 | 0.110 | 0.214 | 74.73 ± 9.62 | 20.86 ± 4.62 | 0.101 | 0.242 |
| | Capture | 97.73 ± 1.32 | 15.86 ± 1.26 | 0.111 | 0.215 | 90.98 ± 9.87 | 12.40 ± 2.95 | 0.052 | 0.109 |
| DW | Air | 86.42 ± 7.07 | 9.43 ± 6.40 | 0.102 | 0.110 | 82.49 ± 22.58 | 12.19 ± 7.09 | 0.054 | 0.110 |

322

323 Net energy recovery (NER) was evaluated for both systems, which achieved comparable NER_V and
324 NER_S values (Figure 5). The best performance in terms of NER in the MFC-PBR system was
325 achieved in Test 3 (0.131 kWh m^{-3} and $0.285 \text{ kWh kgCOD}^{-1}$ removed, respectively), while the lowest
326 performance was obtained in the 24/0 light sequence, CO_2 -capture configuration. While NER_V does
327 not highlight any coherent pattern in the data, an analysis of NER_S data shows that, in tests under
328 PBR-air configuration, MFC2 overcame MFC1 (except for the very first test). Comparing NER_S plot
329 with ηCOD 's in the first phase with synthetic wastewater, both COD removal efficiency and power
330 production were higher for MFC1, explaining why this specific indicator value is lower. In the second
331 phase with DW as anolyte, ηCOD is higher for MFC2 under two out of three conditions tested (16/8
332 and 12/12 light sequence), meaning that under these conditions energy recovery is more efficient in
333 the microalgal cathodic configuration. This information is further confirmed by the volumetric
334 normalized indicator, higher than that reported for MFC1, proving that a PBR-biocathode could be
335 beneficial for energy production when using raw DW wastewater as anolyte.

336



337

338 **Figure 5** - NER_s (a) and NER_v (b) throughout the first phase of the study.

339

340 In the second phase, with DW as feed, energy recovery decreased significantly, achieving values
 341 lower than in the second period of phase one (figure S2, supplementary info). The maximum NER_v
 342 value reached in CO₂-capture configuration (MFC2) was 0.041 kWh m⁻³, while in PBR-air
 343 configuration (MFC1) was 0.061 kWh m⁻³. As for NER_s , MFC2 maximum value reached 0.092 kWh
 344 kgCOD⁻¹, while MFC1's was 0.086 kWh kgCOD⁻¹.

345

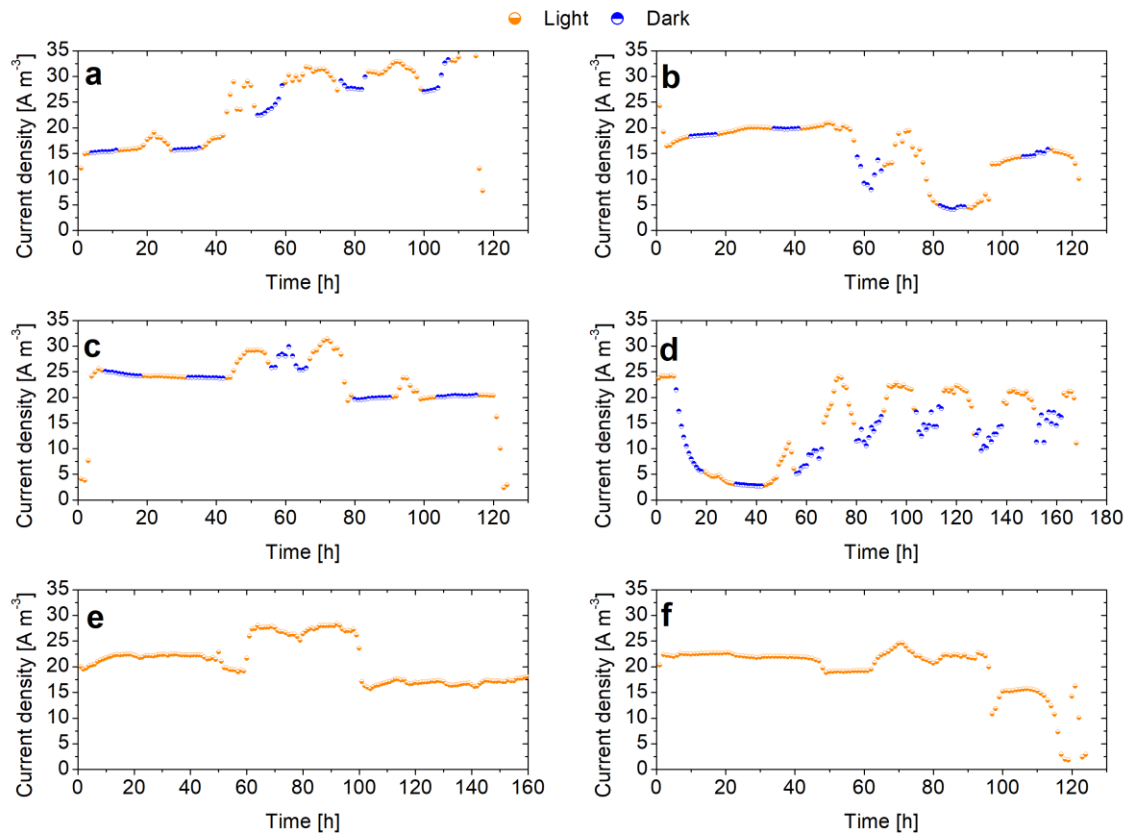
346

3.2 Light/dark ratio and CO₂ availability influence on MFC performance

347 Light/dark sequence affects electricity production, as shown in Figure 6. PBR-air configurations show
348 more stable current productions, even at night-time when algae activity is limited to respiration,
349 consuming oxygen produced during the day. It can be noticed that the 16/8 PBR-aerated operation
350 (Figure 6.a) is the best in terms of current density production (maximum density 39.18 Am^{-3}), with
351 an overall growing trend and low reduction in dark conditions. Under CO_2 -capture configuration and
352 12/12 light/dark sequence (Figure 6.d) more stable current output conditions are reached, with current
353 production up to 24.13 Am^{-3} , decreasing in dark conditions. Under 24/0 sequence (Figure 6.e, f),
354 current production is quite stable under light, due to consistent availability of TEA; however, after
355 four days of operation the CO_2 -capture configuration (Figure 6.f) shows decreasing energy
356 production, due to excessive algal stress, causing inhibition of algal activity.

357 Unfortunately, in tests with DW these differences were less consistently detectable due to variable
358 nature of the substrate, leading to some unpredictability in results (voltage drops were sometimes
359 linked to obstructions in feeding/recirculation lines, in addition to the varying quality of the substrate).

360 Day/night behavior with DW is represented in Figure S4 [SI].



361

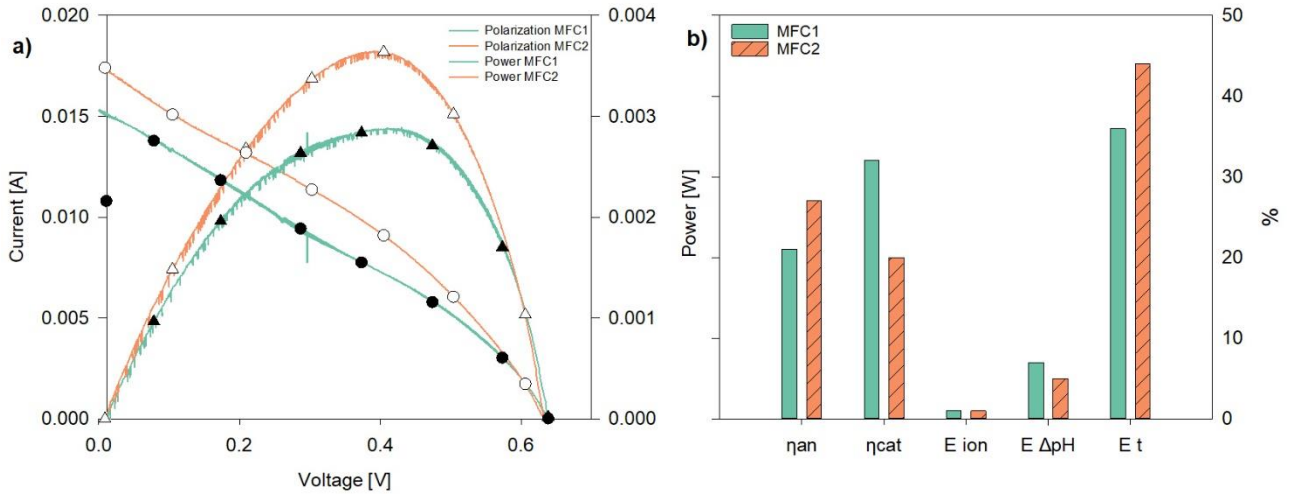
362 **Figure 6** – MFC2 performance under different light/dark sequence with acetate as feeding substrate:
 363 a) 16/8 with PBR-air; b) 16/8 with CO₂-capture; c) 12/12 with PBR-air; d) 12/12 with CO₂-capture;
 364 e) 24/0 with PBR-air; f) 24/0 with CO₂-capture.

365

366 4. Energy losses: differences in PBR-air and CO₂-capture setups

367 Energy losses represent the difference between MFC electromotive force (i.e. theoretical maximum
 368 voltage) and measured voltage at the electrodes. Losses depend on several factors: anode and cathode
 369 overpotentials, membrane overpotentials, pH and conductivity (ionic) gradients are easily detectable
 370 by performing polarization and power curves. Drawing a polarization curve is an important diagnostic
 371 method through which MFC performance efficiency can be assessed, determining also the best
 372 external resistance (R_{ext}) value to achieve a MFC's maximum performance, for example applying the
 373 maximum power point tracking (MPPT) technique (Molognoni et al., 2014). Different strategies can
 374 be used to overcome or mitigate the problem of energy losses, maximizing energy recovery.

375 An example of polarization curve performed during the experimentation is shown in figure 7.



376

377 **Figure 7** – a) Example of polarization and power curve (day 28). Orange: MFC1, green: MFC2.

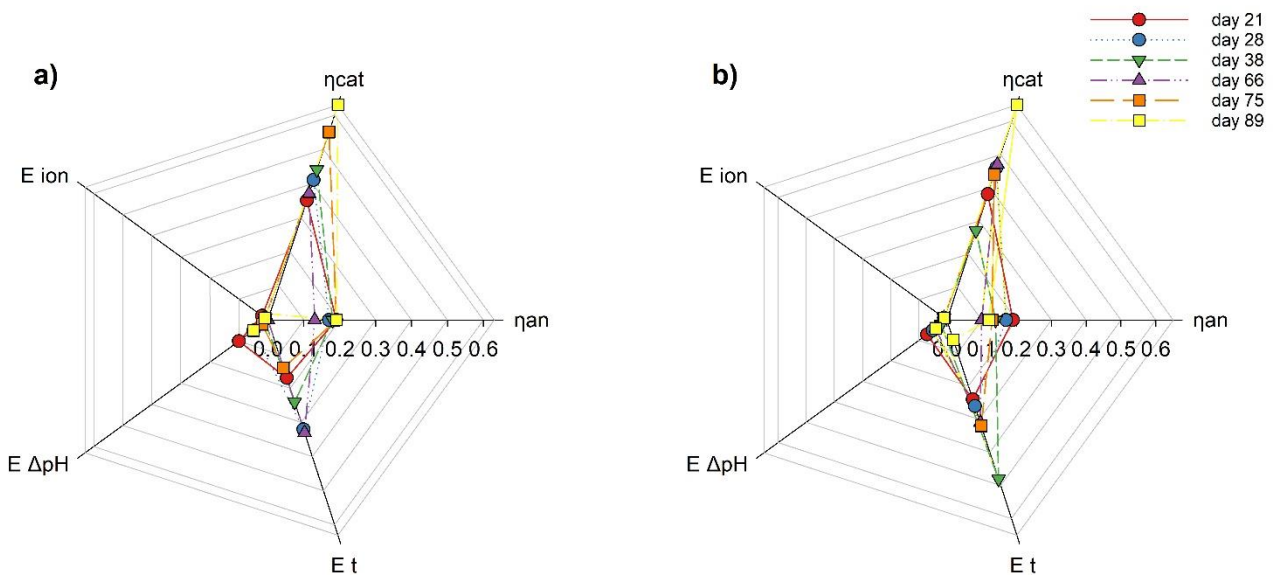
378 Triangles highlight power curves, dots polarization curves. b) Distribution of energy losses at day 28.

379

380 In the present study, it was determined that cathode overpotentials accounted on average for 45% of
381 MFC1's losses, 44% of MFC2's, while membrane overpotentials for 22% in the PBR-air
382 configuration, and 31% in the CO₂-capture configuration. Anodic overpotential and pH gradient only
383 moderately affected energy losses balance. Low pH gradients (between anode and cathode chambers)
384 of maximum one pH unit granted lower losses (less than 10%) than in previous experiences, where
385 significantly higher losses (23%, 2 pH-units) were detected (Molognoni et al., 2018). Anode
386 overpotential accounted on average for 15% of total losses in both MFCs, while electrolyte
387 overpotentials (E_{ion}) could be considered negligible, representing less than 1% of overall losses, due
388 to low difference in conductivity between anode and cathode media ($1.3 \pm 0.4 \text{ mS cm}^{-1}$ for anolyte,
389 $2.6 \pm 0.5 \text{ mS cm}^{-1}$ for catholyte). Anodic overpotential may be caused by increased methanogenic
390 community activity. Comparing the first and the second phases' anodic influents, it can be noticed
391 that pH values increased in the latter, reaching pH up to 8, a value suitable for development of a
392 methanogenic biomass, although no microbial analysis were performed to confirm this hypothesis.
393 Feeding an influent with lower pH, pH-gradient related losses would increase; these could be reduced

394 by modifying the system's hydraulic retention time, or by varying its design. Data collected in this
 395 phase for MFC1 and MFC2 are reported in Figure 8.

396 As reported in literature, cathode overpotentials may be reduced by: (i) introducing new, more
 397 efficient electrode and catalyzer materials; (ii) improving oxygen transfer kinetics at the cathode; (iii)
 398 developing a biocathode. Algal biocathodes, as shown from experimental data of this study, seem to
 399 reduce electron transfer efficiency, due to increase in membrane and electrode fouling. However, no
 400 significant difference in cathode overpotential was detected between the unit purged with air and the
 401 one relying only on anodic CO_2 conversion. Membrane overpotentials could be reduced by
 402 introducing different materials characterized by lower internal resistance, or less subject to
 403 biofouling.



404
 405 **Figure 8** – Energy losses in MFC1 (a) and MFC2 (b), respectively.

406

407 **5. Energy and circular economy considerations**

408 Few authors explored the possibility of coupling MFC and microalgae. Table 4 reports a summary of
 409 studies found in literature, allowing a comparison between the present work and other experiences. It
 410 is possible to notice that the system configuration used in this study overcame other architectures'
 411 power productions.

412

413 **Table 4** – Reported studies of MFC with microalgae.

| MFC type | Influent type | Power production | CE [%] | η COD [%] | Microalgal species | Ref. |
|--------------------------|---------------|--|--------|------------------------|--------------------|---------------------------------------|
| Two chambers | LL + MW | 0.517 W m ⁻³ 0.050 W m ⁻² | - | 96.8 (A) 0÷56.8 (C) | Not specified | (Nguyen et al., 2017) |
| Tubular, external PBR | MW (diluted) | 0.006 W m ⁻² | - | 80.8 | <i>Chlorella</i> | (Kakarla and Min, 2019) |
| Two chambers | SUW | 0.031 W m ⁻² | <1 | 40.0÷90.0 | <i>C. vulgaris</i> | (Gonzalez et al., 2015) |
| Tubular | MW | 0.124 W m ⁻³ | 57÷78 | 4.1÷5.5 | <i>C. vulgaris</i> | (Bazdar et al., 2018) |
| Two chambers + PBR | AC | 2.8 ± 0.9 W m ⁻³ | 16 ± 5 | 65.3÷97.2 | <i>Chlorella</i> | Present study, first phase (AC) |
| Two chambers + PBR | DW | 1.9 ± 0.5 W m ⁻³ | 9 ± 4 | 56.1÷98.1 | <i>Chlorella</i> | Present study, first phase (DW) |
| Two chambers + PBR | DW | 2.5 ± 0.4 W m ⁻³ | 7 ± 3 | 85.5 ÷ 99.9 | <i>Chlorella</i> | Present study, second phase |

414 AC: acetate; DW: dairy wastewater; LL: landfill leachate; MW: municipal wastewater; SUW: synthetic urban
 415 wastewater.

416

417 Using microalgae as oxygen providers in a MFC system can improve its overall energy balance by
 418 decreasing the cost of aeration for TEA supply. The presence of microalgae can also improve the
 419 overall energy and economic balance of waste substrate treatment, by exploiting different materials
 420 and biofuels precursors potentially recoverable from conversion of algal biomass. Liquid biofuels,
 421 e.g. biodiesel, bioethanol, biobutanol and jet fuels, are the most likely outcomes of algal biorefining
 422 (Dasan et al., 2019; Liang et al., 2015). Biodiesel may be obtained from oil extraction and following
 423 transesterification, with properties complying with EU specifications, bioethanol and biobutanol may
 424 be derived from algae fermentation processes (Callegari et al., 2020), while biochar may be obtained
 425 by thermal treatment (Yu et al., 2017). One of the major challenges with microalgae is to achieve
 426 efficient and inexpensive oil extraction (Chiew and Shimada, 2013). International regulations and
 427 shrinking of fossil fuels reserves will expand the renewable energy market in the next decades. Algal
 428 biomass has been indicated as a major component of the future eco-fuel panorama (Callegari et al.,
 429 2020), even though, considering current market prices of liquid biofuels, they are still not an

430 economically appealing solution per se, with production costs higher than traditional fossil fuels.
431 Lundquist et al., in fact estimated the cost of large scale production of algae-derived oil from
432 wastewater at 332 \$ per barrel when focusing on oil production alone; however, when considering
433 wastewater treatment as the main focus, with algal biomass recovered as a by-product precursor of
434 oil, the calculated cost of algae-derived oil would drop to 28 \$ per barrel (lower than the average cost
435 of crude oil) (Lundquist et al., 2010).

436 Microalgae can also be considered a feedstock for chemicals and materials recovery, such as slow-
437 release fertilizers, since they are capable of accumulating surplus quantities of nutrients, recoverable
438 as dried microalgal biomass or biochar from pyrolysis (Bolognesi et al., 2019). Biofertilizers and
439 biostimulants appear to be one of the most economically appealing fields in algal technology, with
440 market prices in the range of 9-23 € kg⁻¹ for biostimulants, and 0.2-0.5 € kg⁻¹ for biofertilizers (Voort
441 et al., 2015). Anticipated climatic changes and increasing costs of fertilizers due to reserve shortages
442 (Daneshgar et al., 2018) will open the agronomy field to new green biostimulants development.

443 Finally, the nutritional value of microalgae could open the possibility for their use in the food and
444 feed (aquaculture or livestock) market, however, food, feed and pharmaceutical reuse of algae grown
445 in wastewater treatment processes still present issues of social acceptance; so far, the most favorable
446 market outlets for microalgae recovery consist of biofuels production, biofertilizers and soil
447 amendment products.

448

449 **6. Conclusions**

450 This study aimed at evaluating the performance of an MFC-PBR system treating synthetic (acetate
451 and real (dairy wastewater) substrates with energy biorecovery under different operational conditions,
452 and to establish optimal process configuration. Two systems of identical base configuration were
453 operated continuously for up to 60 days at a time, using the same substrate as feed, but using different
454 TEA supply methods. Both systems proved to be effective for wastewater treatment (COD removal),
455 and showed higher power density generation than similar systems described in literature studies.

456 However, concerning bioelectricity production, a traditional system proved to be more stable and
457 better performing than the MFC-PBR under almost every condition tested, when using synthetic
458 substrate. Systems' performance gap reduced when passing from synthetic substrate to real
459 wastewater feed, showing increasing performance of the MFC-PBR unit, as confirmed by the relative
460 increase of NER_S and NER_V , compared to the same parameters in the conventional unit. This fact
461 was attributed to greater substrate complexity slowing down the anodic reactions in the better
462 performing system, reducing the limiting influence of microalgal metabolism on cathodic activity.
463 This indicates that MFC-PBR combination systems with microalgae may become a feasible option
464 for sustainable wastewater treatment, when the key limitations of MFC will be solved.
465 Despite many efforts to increase these systems efficiency, in fact, the major issue in MFC technology
466 is linked to internal energy losses, impairing net energy production and recovery, which unfortunately
467 was not sufficiently improved by the introduction of algae as oxygen (TEA) providers. Several
468 existing and envisioned possibilities of recovery and valorization of algal effluent, however, could
469 help improve the overall economic and energetic balance of these system, at the same time reducing
470 their atmospheric CO₂ impact.

471

472 **Acknowledgements**

473 Silvia Bolognesi is a Ph.D. candidate at the University of Pavia, subsequently admitted to a Double
474 Doctorate program at the University of Girona. The study herein described was carried out at the
475 University of Pavia. The source of the wastewater used for experiments is not disclosed due to an
476 explicit request of the supplying company. The authors thank Salvatore Orani and Nicola Gentile
477 for their help in collecting the data in the first and second phase of the experimentation.

478

479

480 **References**

481 Arndt, D.S., Baringer, M.O., Johnson, M.R., 2010. State of the climate in 2009. Bull. Amer.

482 Meteor. Soc., 91 (7), S1–S224

483 Bazdar, E., Roshandel, R., Yaghmaei, S., Mahdi, M., 2018. The effect of different light intensities
484 and light/dark regimes on the performance of photosynthetic microalgae microbial fuel cell.
485 Bioresour. Technol. 261, 350–360. <https://doi.org/10.1016/j.biortech.2018.04.026>

486 Bolognesi, S., Bernardi, G., Callegari, A., Dondi, D., Capodaglio, A.G., 2019. Biochar production
487 from sewage sludge and microalgae mixtures: properties, sustainability and possible role in
488 circular economy. Biomass Convers. Biorefinery. <https://doi.org/10.1007/s13399-019-00572-5>

489 Bolognesi, S., Cecconet, D., Callegari, A., Capodaglio, A.G., 2020. Bioelectrochemical treatment of
490 municipal solid waste landfill mature leachate and dairy wastewater as co-substrates. Environ.
491 Sci. Pollut. Res. <https://doi.org/10.1007/s11356-020-10167-7>

492 Brennan, L., Owende, P., 2010. Biofuels from microalgae-A review of technologies for production,
493 processing, and extractions of biofuels and co-products. Renew. Sustain. Energy Rev. 14, 557–
494 577. <https://doi.org/10.1016/j.rser.2009.10.009>

495 Callegari, A., Bolognesi, S., Cecconet, D., Capodaglio, A.G., 2020. Production technologies,
496 current role, and future prospects of biofuels feedstocks: a state-of-the-art review. Crit. Rev.
497 Environ. Sci. Technol. 50, 384–436. <https://doi.org/10.1080/10643389.2019.1629801>

498 Capodaglio, A.G., Molognoni, D., Dallago, E., Liberale, A., Cella, R., Longoni, P., Pantaleoni, L.,
499 2013. Microbial fuel cells for direct electrical energy recovery from urban wastewaters. Sci.
500 World J. 2013. <https://doi.org/10.1155/2013/634738>

501 Capodaglio, A.G., Molognoni, D., Pons, A.V., 2016. A multi-perspective review of microbial fuel-
502 cells for wastewater treatment: Bio-electro-chemical, microbiologic and modeling aspects. AIP
503 Conf. Proc. 1758. <https://doi.org/10.1063/1.4959428>

504 Capodaglio, A.G., Molognoni, D., Puig, S., Balaguer, M.D., Colprim, J., 2015. Role of operating
505 conditions on energetic pathways in a Microbial Fuel Cell. Energy Procedia 74, 728–735.
506 <https://doi.org/10.1016/j.egypro.2015.07.808>

507 Capodaglio, A.G., Olsson, G., 2020. Energy Issues in Sustainable Urban Wastewater Management:

508 Use, Demand Reduction and Recovery in the Urban Water Cycle. *Sustainability* 12.
509 <https://doi.org/10.3390/su12010266>

510 Ceconet, D., Bolognesi, S., Molognoni, D., Callegari, A., Capodaglio, A.G., 2018. Influence of
511 reactor's hydrodynamics on the performance of microbial fuel cells. *J. Water Process Eng.* 26,
512 281–288. <https://doi.org/10.1016/j.jwpe.2018.10.019>

513 Cherubini, F., 2010. The biorefinery concept : Using biomass instead of oil for producing energy
514 and chemicals. *Energy Convers. Manag.* 51, 1412–1421.
515 <https://doi.org/10.1016/j.enconman.2010.01.015>

516 Chew, K.W., Yap, J.Y., Show, P.L., Suan, N.H., Juan, J.C., Ling, T.C., Lee, D.J., Chang, J.S., 2017.
517 Microalgae biorefinery: High value products perspectives. *Bioresour. Technol.* 229, 53–62.
518 <https://doi.org/10.1016/j.biortech.2017.01.006>

519 Chiew, Y.L., Shimada, S., 2013. Current state and environmental impact assessment for utilizing oil
520 palm empty fruit bunches for fuel, fiber and fertilizer - A case study of Malaysia. *Biomass and*
521 *Bioenergy* 51, 109–124. <https://doi.org/10.1016/j.biombioe.2013.01.012>

522 Cui, Y., Rashid, N., Hu, N., Saif, M., Rehman, U., Han, J., 2014. Electricity generation and
523 microalgae cultivation in microbial fuel cell using microalgae-enriched anode and bio-cathode.
524 *Energy Convers. Manag.* 79, 674–680. <https://doi.org/10.1016/j.enconman.2013.12.032>

525 Daneshgar, S., Callegari, A., Capodaglio, A.G., Vaccari, D., 2018. The Potential Phosphorus Crisis:
526 Resource Conservation and Possible Escape Technologies: A Review. *Resources* 7.
527 <https://doi.org/10.3390/resources7020037>

528 Do, M.H., Ngo, H.H., Guo, W.S., Liu, Y., Chang, S.W., Nguyen, D.D., Nghiem, L.D., Ni, B.J.,
529 2018. Challenges in the application of microbial fuel cells to wastewater treatment and energy
530 production: A mini review. *Sci. Total Environ.* 639, 910–920.
531 <https://doi.org/10.1016/j.scitotenv.2018.05.136>

532 Gabriel, F., Fernández, A., Gómez-serrano, C., 2018. Recovery of Nutrients From Wastewaters
533 Using Microalgae. *Front. Sustain. Food Syst.* 2, 1–13.

534 <https://doi.org/10.3389/fsufs.2018.00059>

535 Ge, Z., Li, J., Xiao, L., Tong, Y., He, Z., 2014. Recovery of Electrical Energy in Microbial Fuel
536 Cells. *Environ. Sci. Technol. Lett.* 1, 137–141. <https://doi.org/10.1021/ez4000324>

537 Goglio, A., Tucci, M., Rizzi, B., Colombo, A., Cristiani, P., Schievano, A., 2019. Microbial
538 recycling cells (MRCs): A new platform of microbial electrochemical technologies based on
539 biocompatible materials, aimed at cycling carbon and nutrients in agro-food systems. *Sci.*
540 *Total Environ.* 649, 1349–1361. <https://doi.org/10.1016/j.scitotenv.2018.08.324>

541 Gonzalez, A., Perez, J.F., Cañizares, P., Rodrigo, M.A., Fernandez, F.J., Lobato, J., 2015.
542 Characterization of light / dark cycle and long-term performance test in a photosynthetic
543 microbial fuel cell. *FUEL* 140, 209–216. <https://doi.org/10.1016/j.fuel.2014.09.087>

544 Gouveia, L., Neves, C., Sebastião, D., Nobre, B.P., Matos, C.T., 2014. Effect of light on the
545 production of bioelectricity and added-value microalgae biomass in a Photosynthetic Alga
546 Microbial Fuel Cell. *Bioresour. Technol.* 154, 171–177.
547 <https://doi.org/10.1016/j.biortech.2013.12.049>

548 Jiang, H., Luo, S., Shi, X., Dai, M., Guo, R., 2013. A system combining microbial fuel cell with
549 photobioreactor for continuous domestic wastewater treatment and bioelectricity generation. *J.*
550 *Cent. South Univ.* 20, 488–494. <https://doi.org/10.1007/s11771-013-1510-2>

551 Kakarla, R., Min, B., 2019. Sustainable electricity generation and ammonium removal by microbial
552 fuel cell with a microalgae assisted cathode at various environmental conditions. *Bioresour.*
553 *Technol.* 284, 161–167. <https://doi.org/10.1016/j.biortech.2019.03.111>

554 Kanna Dasan, Y., Kee Lam, M., Yusup, S., Wei Lim, J., Teong Lee, K., 2019. Life cycle evaluation
555 of microalgae biofuels production: Effect of cultivation system on energy, carbon emission and
556 cost balance analysis. *Sci. Total Environ.* 688, 112–128.
557 <https://doi.org/10.1016/j.scitotenv.2019.06.181>

558 Khazraee Zamanpour, M., Kariminia, H.R., Vosoughi, M., 2017. Electricity generation,
559 desalination and microalgae cultivation in a biocathode-microbial desalination cell. *J. Environ.*

560 Chem. Eng. 5, 843–848. <https://doi.org/10.1016/j.jece.2016.12.045>

561 Kothari, R., Pandey, A., Ahmad, S., Kumar, A., Pathak, V. V., Tyagi, V. V., 2017. Microalgal
562 cultivation for value-added products: a critical enviro-economical assessment. 3 Biotech 7, 1–
563 15. <https://doi.org/10.1007/s13205-017-0812-8>

564 León-Vaz, A., León, R., Díaz-Santos, E., Vígara, J., Raposo, S., 2019. Using agro-industrial wastes
565 for mixotrophic growth and lipids production by the green microalga *Chlorella sorokiniana*. N.
566 Biotechnol. 51, 31–38. <https://doi.org/10.1016/j.nbt.2019.02.001>

567 Liang, Y., Kashdan, T., Sterner, C., Dombrowski, L., Petrick, I., Kröger, M., Höfer, R., 2015. Algal
568 Biorefineries, Industrial Biorefineries and White Biotechnology. [https://doi.org/10.1016/B978-](https://doi.org/10.1016/B978-0-444-63453-5.00002-1)
569 [0-444-63453-5.00002-1](https://doi.org/10.1016/B978-0-444-63453-5.00002-1)

570 Logan, B.E., Hamelers, B., Rozendal, R., Schröder, U., Keller, J., Freguia, S., Aelterman, P.,
571 Verstraete, W., Rabaey, K., 2006. Microbial fuel cells: Methodology and technology. Environ.
572 Sci. Technol. 40, 5181–5192. <https://doi.org/10.1021/es0605016>

573 Logan, B.E., Rabaey, K., 2013. Conversion of Waste into Bioelectricity and Chemical by Using
574 Microbial Electrochemical Technologies. Science (80-.). 337, 686–690.

575 Lundquist, T., Woertz, I., Quinn, N., Benemann, J., 2010. A Realistic Technology and Engineering
576 Assessment of Algae Biofuel Production. University of California.

577 Luo, S., Berges, J.A., He, Z., Young, E.B., 2017. Algal-microbial community collaboration for
578 energy recovery and nutrient remediation from wastewater in integrated
579 photobioelectrochemical systems. Algal Res. 24, 527–539.
580 <https://doi.org/10.1016/j.algal.2016.10.006>

581 McCarty, P.L., Bae, J., Kim, J., 2011. Domestic wastewater treatment as a net energy producer-can
582 this be achieved? Environ. Sci. Technol. 45, 7100–7106. <https://doi.org/10.1021/es2014264>

583 Molognoni, D., Chiarolla, S., Cecconet, D., Callegari, A., Capodaglio, A.G., 2018. Industrial
584 wastewater treatment with a bioelectrochemical process: Assessment of depuration efficiency
585 and energy production. Water Sci. Technol. 77, 134–144. <https://doi.org/10.2166/wst.2017.532>

586 Molognoni, D., Puig, S., Balaguer, M.D., Capodaglio, A.G., Callegari, A., Colprim, J., 2016.
587 Multiparametric control for enhanced biofilm selection in microbial fuel cells. *J. Chem.*
588 *Technol. Biotechnol.* 91, 1720–1727. <https://doi.org/10.1002/jctb.4760>

589 Molognoni, D., Puig, S., Balaguer, M.D., Liberale, A., Capodaglio, A.G., Callegari, A., Colprim, J.,
590 2014. Reducing start-up time and minimizing energy losses of Microbial Fuel Cells using
591 Maximum Power Point Tracking strategy. *J. Power Sources* 269, 403–411.
592 <https://doi.org/10.1016/j.jpowsour.2014.07.033>

593 Nguyen, H.T.H., Kakarla, R., Min, B., 2017. Algae cathode microbial fuel cells for electricity
594 generation and nutrient removal from landfill leachate wastewater. *Int. J. Hydrogen Energy* 42,
595 29433–29442. <https://doi.org/10.1016/j.ijhydene.2017.10.011>

596 Nguyen, H.T.H., Min, B., 2020. Leachate treatment and electricity generation using an algae-
597 cathode microbial fuel cell with continuous flow through the chambers in series. *Sci. Total*
598 *Environ.* 723, 138054. <https://doi.org/10.1016/j.scitotenv.2020.138054>

599 Puig, S., Serra, M., Vilar-Sanz, A., Cabré, M., Bañeras, L., Colprim, J., Balaguer, M.D., 2011.
600 Autotrophic nitrite removal in the cathode of microbial fuel cells. *Bioresour. Technol.* 102,
601 4462–4467. <https://doi.org/10.1016/j.biortech.2010.12.100>

602 Richmond, A., 2004. *Handbook of Microalgal Culture: biotechnology and applied phycology.*
603 Blackwell Science Ltd.

604 Rosso, D., Stenstrom, M.K., 2008. The carbon-sequestration potential of municipal wastewater
605 treatment. *Chemosphere* 70, 1468–1475.
606 <https://doi.org/https://doi.org/10.1016/j.chemosphere.2007.08.057>

607 Sabba, F., Terada, A., Wells, G. et al. Nitrous oxide emissions from biofilm processes for
608 wastewater treatment. *Appl Microbiol Biotechnol* 102, 9815–9829 (2018).
609 <https://doi.org/10.1007/s00253-018-9332-7>

610 Sleutels, T.H.J.A., Hamelers, H.V.M., 2009. Ion transport resistance in Microbial Electrolysis Cells
611 with anion and cation exchange membranes. *Int. J. Hydrogen Energy* 34, 3612–3620.

612 <https://doi.org/10.1016/j.ijhydene.2009.03.004>

613 US DOE, 2014. The Water-Energy Nexus: Challenges and Opportunities. US Department of
614 Environment, Washington DC.

615 Voort, M.P.J. Van Der, Vulsteke, E., Visser, C.L.M. de., 2015. Macro-economics of algae products.
616 Public output report of the EnAlgae project, Swansea, June 2015.

617 Wang, X., Feng, Y., Liu, J., Lee, H., Li, C., Li, N., Ren, N., 2010. Sequestration of CO₂ discharged
618 from anode by algal cathode in microbial carbon capture cells (MCCs). *Biosens. Bioelectron.*
619 25, 2639–2643. <https://doi.org/10.1016/j.bios.2010.04.036>

620 Wang, X., Tian, Y., Liu, H., Zhao, X., Peng, S., 2019. The influence of incorporating microbial fuel
621 cells on greenhouse gas emissions from constructed wetlands. *Sci. Total Environ.* 656, 270–
622 279. <https://doi.org/10.1016/j.scitotenv.2018.11.328>

623 Xia, X., Tokash, J.C., Zhang, F., Liang, P., Huang, X., Logan, B.E., 2013. Oxygen-Reducing
624 Biocathodes Operating with Passive Oxygen Transfer in Microbial Fuel Cells. *Environ. Sci.*
625 *Technol.* 47, 2085–2091. <https://doi.org/dx.doi.org/10.1021/es3027659>.

626 Yu, K.L., Show, P.L., Ong, H.C., Ling, T.C., Chi-Wei Lan, J., Chen, W.H., Chang, J.S., 2017.
627 Microalgae from wastewater treatment to biochar – Feedstock preparation and conversion
628 technologies. *Energy Convers. Manag.* 150, 1–13.
629 <https://doi.org/10.1016/j.enconman.2017.07.060>

630